

UC Santa Barbara

Recent Work

Title

Moments and Probability Density Functions in Turbulent Boundary Layers

Permalink

<https://escholarship.org/uc/item/770564zd>

Authors

Birnir, Bjorn

Chen, Xi

Can, Liu

Publication Date

2015-08-26

Moments and Probability Density Functions in Turbulent Boundary Layers

Björn Birnir, CNLS and Department of Mathematics
UC Santa Barbara
and

Xi Chen and Can Liu, Department of Mechanical Engineering
Texas Tech University, TX, 79409-1021, USA

August 22, 2015

1 Introduction

Turbulent boundary layers are important for high-Reynolds number flow in applications. In many physical situations flows dominated by inertia interact with solid boundaries, these may be the wings of the aircraft, the blades inside a jet engine or the ground or the ocean's surface on windfarms. The famous log-law of Prandtl [27] and von Kármán [35] is the most distinguished characteristic of such flows. It says that the mean-velocity profile in the inertial region of the flow satisfies the formula:

$$\langle u \rangle / u_\tau = \kappa^{-1} \ln(yu_\tau/\nu) + B, \quad (1)$$

where $u_\tau = \sqrt{\tau_w/\rho}$ is the friction velocity based on the wall stress τ_w , ρ is the fluid density, ν is the kinematic viscosity, κ is the von Kármán constant and B is also a constant. The log-law is well established both experimentally and numerically, see reviews by Smits, McKeon and Marusic [33] and Jimenez [14]. It has proven to be an invaluable tool in the theory of turbulent boundary layers.

In recent year a number of authors Marusic and Kunkel [18], Hultmark et al. [12] and Marusic [17] and Marusic et al. [20] have proposed a universal law of the form

$$\langle (u')^2 \rangle / u_\tau^2 = B_1 - A_1 \ln(y/\delta) \quad (2)$$

for the streamwise fluctuations $u' = u - \langle u \rangle$, motivated by the "attached eddy hypothesis" of Townsend [34], Perry and Chong [25] and Perry, Henbest and Chong [26]. δ is the height of the boundary layer or the channel, or in case of pipe flow, the radius of the pipe. A_1 is a universal constant but B_1 is supposed to depend on the particular flow geometry.

It was suggested by Meneveau and Marusic [19] that the log-law of the second moment of the fluctuations (2) could be generalized to any moment $p \geq 2$ by the law

$$\langle (u')^{2p} \rangle^{1/p} = B_p - A_p \ln(y/\delta) = D_p(Re_\tau) - A_p \ln(y^+) \quad (3)$$

where $y^+ = yu_\tau/\nu$ are the viscous units and $D_p = B_p + A_p \ln Re_\tau$ is a Reynolds number Re_τ dependent offset.

In this paper we will extend the theory of Birnir [5, 6] developed for homogeneous turbulence to boundary layers to prove (3) with a physically-based normalization in the inertial range. We will show that the universal constants satisfy the relationship

$$A_p = \left(\frac{1}{l^*} \right)^{\zeta_1 - \zeta_p/p} \frac{C_p^{1/p}}{C_1} A_1$$

where $\zeta_p = p/3 + \tau_p = p/9 + 2(1 - (2/3)^{p/3})$ are the Kolmogorov-Obukhov-She-Leveque (KOSL), scaling exponents of the structure functions of turbulence, see [6], and l^* is a small constant. The coefficients C_p are the Kolmogorov-Obukhov scaling coefficients computed in [5, 6], and in Section 3. These coefficients are not universal for general turbulent flows, as pointed out by Landau [15], [23], for example the coefficients for channel flow will be different from those for pipe-flow. However, the coefficients may be universal for pipe flow. The sub-Gaussian behavior of the A_p s is caused by the KOSL scaling. We will in fact show that if A_1 is finite then the A_p s are finite for finite p :

$$\sup A_p \leq b\sqrt{p}A_1, \quad (4)$$

where b is a constant, for p sufficiently large. However, $\lim_{p \rightarrow \infty} \sup A_p = \infty$.

We also compute the probability density functions of the fluctuations in the inertial range and in the viscous range. In the inertial range the PDFs turn out to be Generalized Hyperbolic Distributions multiplied by a discrete measure, see [8]. In the viscous range the PDFs are skewed Gaussians, analogous to the moments of turbulent velocity, see Batchelor [2].

2 The Deterministic Navier-Stokes Equations

A general incompressible fluid flow satisfies the Navier-Stokes Equation

$$u_t + u \cdot \nabla u = \nu \Delta u - \nabla p, \quad u(x, 0) = u_0(x)$$

with the incompressibility condition $\nabla \cdot u = 0$. Eliminating the pressure using the incompressibility condition gives

$$u_t + u \cdot \nabla u = \nu \Delta u + \nabla \Delta^{-1} \text{trace}(\nabla u)^2, \quad u(x, 0) = u_0(x).$$

The turbulence is quantified by the dimensionless Taylor-Reynolds number $Re_\lambda = \frac{U\lambda}{\nu}$ [28].

2.1 Reynolds Decomposition

Following the classical Reynolds decomposition [29], we decompose the velocity into mean flow U and the fluctuations u . Then the velocity is written as $U + u$, where U describes the large scale flow and u describes the small scale turbulence. We must also decompose the pressure into mean pressure P and the fluctuations p , then the equation for the large scale flow can be written as

$$U_t + U \cdot \nabla U = \nu \Delta U - \nabla P - \nabla \cdot (\overline{u \otimes u}), \quad (5)$$

where in coordinates $\nabla \cdot (\overline{u \otimes u}) = \frac{\partial \overline{u_i u_j}}{\partial x_j}$, that is ∇ is dotted with the rows of $\overline{u_i u_j}$ and $R_{ij} = \overline{u \otimes u}$ is the Reynolds stress, see [3]. The Reynolds stress has the interpretation of a turbulent momentum flux and the last term in (5) is also known as the eddy viscosity. It describes how the small scales influence the large scales. In addition we get divergence free conditions for U , and u

$$\nabla \cdot U = 0, \quad \nabla \cdot u = 0.$$

Together, (5) and the divergence free condition on U give Reynolds Averaged Navier-Stokes (RANS) that forms the basis for most contemporary simulations of turbulent flow.

Finding a constitutive law for the Reynolds stress $\overline{u \otimes u}$ is the famous closure problem in turbulence and we will solve that by writing down a stochastic equation for the small scale velocity u . The hypothesis is that the large scales influence the small scales directly, through the fluid instabilities and the noise in fully developed

turbulence. An example of this mechanics, how the instabilities magnify the tiny ambient noise to produce large noise, is given in [4], see also Chapter 1 in [6].

Now consider the inertial range in turbulence. In Fourier space this is the range of wave numbers k : $\frac{1}{L} \leq |k| \leq \frac{1}{\eta}$, where $\eta = (\nu^3/\varepsilon)^{1/4}$ is the Kolmogorov length scale, ε is the energy dissipation and L the size of the largest eddies, see [6]. If we assume that dissipation takes place on all length scale in the inertial range then the form of the dissipation processes are determined by the fundamental theorems of probability. Namely, if we impose periodic boundary conditions (different boundary conditions correspond to different basis vectors), then the (functional) central limit theorem and the large deviation principle stipulate that the additive noise in the Navier-Stokes equation for the small scale must be of the form:

$$\sum_{k \neq 0} c_k^{\frac{1}{2}} db_t^k e_k(x) + \sum_{k \neq 0} d_k |k|^{1/3} dt e_k(x),$$

where $e_k(x) = e^{2\pi i k \cdot x}$ are the Fourier coefficient and $c_k^{\frac{1}{2}}$ and d_k are coefficients that ensure the series converge in 3 dimensions. The first term describes the mean of weakly coupled dissipation processes given by the central limit theorem and the second term describes the large deviations of that mean, given by the large deviation principle, see [6]. Thus together the two terms give a complete description of the mean of the dissipation process similar to the mean of many processes in probability. The factor $|k|^{1/3}$ implies that the mean dissipation has only one scaling. The Fourier coefficients of the first series contain independent Brownian motions b_t^k and thus the noise is white in time, in the infinitely many directions in function space. The noise cannot be white in space, hence the decaying coefficients $c_k^{1/2}$ and d_k , because if it was the small scale velocity u would be discontinuous in 3 dimension, see [5]. This is contrary to what is observed in nature.

The other part of the noise, in fully developed turbulence, is multiplicative and models the excursion (jumps) in the velocity gradient or vorticity concentrations. If we let N_t^k denote the integer number of velocity excursion, associated with k th wavenumber, that have occurred at time t , so that the differential $dN^k(t) = N^k(t + dt) - N^k(t)$ denotes the number of excursions in the time interval $(t, t + dt]$, then the process $df_t = \sum_{k \neq 0}^M \int_{\mathbb{R}} h_k(t, z) \bar{N}^k(dt, dz)$, gives the multiplicative noise term. One can show that any noise corresponding to jumps in the velocity gradients must have this multiplicative noise to leading order, see [5]. A detailed derivation of both the noise terms can be found in [5] and [6].

Adding the additive noise and the multiplicative noise we get the stochastic

Navier-Stokes equations describing the small scales in fully developed turbulence

$$\begin{aligned}
du = & (\nu\Delta u - u \cdot \nabla u + \nabla\Delta^{-1}\text{tr}(\nabla u)^2)dt + \sum_{k \neq 0} c_k^{\frac{1}{2}} db_t^k e_k(x) + \sum_{k \neq 0} d_k |k|^{1/3} dt e_k(x) \\
(6) \quad & - U \cdot \nabla u - u \cdot \nabla U + u \left(\sum_{k \neq 0} \int_{\mathbb{R}} h_k \bar{N}^k(dt, dz) \right), \quad u(x, 0) = u_0(x),
\end{aligned}$$

where we have used the divergence free condition $\nabla \cdot u = 0$ to eliminate the small scale pressure p . Each Fourier component e_k comes with its own Brownian motion b_t^k and a deterministic bound $|k|^{1/3} dt$. The terms $-U \cdot \nabla u - u \cdot \nabla U$ describe how the large scale flow (5) influences the small scale flow. The small scale equation (6) can now be considered to be a stochastic closure of the large scale equation (5).

2.2 Solution of the Stochastic Navier-Stokes

The next step is to figure out how the generic noise interacts with the Navier-Stokes evolution. This is determined by the integral form of the equation (6),

$$u = e^{Kt} e^{\int_0^t dq} M_t u^0 + \sum_{k \neq 0} \int_0^t e^{K(t-s)} e^{\int_s^t dq} M_{t-s} (c_k^{1/2} db_s^k + d_k |k|^{1/3} ds) e_k(x), \quad (7)$$

where K is the operator $K = \nu\Delta + \nabla\Delta^{-1}\text{tr}(\nabla u \nabla)$, and we have omitted the terms $-U \cdot \nabla u - u \cdot \nabla U$ in (6), to simplify the exposition. (These terms are easily incorporated using the machinery below.) The equation is an implicit solution of the stochastic Navier-Stokes equation (6). We solve (6) using the Feynmann-Kac formula, and using Girsanov's Theorem from probability theory, see [6], to get (7). Girsanov's Theorem gives the Martingale $M_t = \exp\{-\int_0^t u(B_s, s) \cdot dB_s - \frac{1}{2} \int_0^t |u(B_s, s)|^2 ds\}$. The Feynmann-Kac formula gives the exponential of a sum of terms of the form $\int_s^t dq^k = \int_0^t \int_{\mathbb{R}} \ln(1 + h_k) N^k(dt, dz) - \int_0^t \int_{\mathbb{R}} h_k m^k(dt, dz)$, see [5] or [6] Chapter 2 for details. The form of the processes

$$(8) \quad e^{\int_0^t \int_{\mathbb{R}} \ln(1+h_k) N^k(dt, dz) - \int_0^t \int_{\mathbb{R}} h_k m^k(dt, dz)} = e^{N_t^k \ln \beta + \gamma \ln |k|} = |k|^{\gamma \beta} N_t^k$$

was found by She and Leveque [30], for $h_k = \beta - 1$. It was pointed out by She and Waymire [31] and by Dubrulle [10] that they are log-Poisson processes. The upshot of this computation is that we see the Navier-Stokes evolution acting on the additive noise to give the Kolmogorov-Obukhov '41 scaling, and the Navier-Stokes evolution acting on the multiplicative noise to produce the intermittency

corrections through the Feynmann-Kac formula. Together these two scaling combine to give the scaling of the structure functions in turbulence. We will see below how the two scalings separate in the invariant measure to give two distinct contributions to the final scaling.

3 The Kolmogorov-Obukhov-She-Leveque Scaling

The scaling of the structure functions

$$S_p(x, y, t) = E(|u(x, t) - u(y, t)|^p),$$

where E is the expectation, is

$$S_p \sim C_p |x - y|^{\zeta_p}, \quad \zeta_p = \frac{p}{3} + \tau_p = \frac{p}{9} + 2(1 - (2/3)^{p/3}), \quad (9)$$

$\frac{p}{3}$ being the Kolmogorov scaling and τ_p the intermittency corrections. The scaling of the structure functions is consistent with Kolmogorov's 4/5 law,

$$S_3^* = -\frac{4}{5}\varepsilon|x - y|,$$

to leading order, where $\varepsilon = -\frac{d\mathcal{E}}{dt} = 2\nu \int_0^\infty k^2 E(k, t) dk$ is the energy dissipation.¹ S_3^* is the third structure function without absolute values, so it can be negative.

The first structure functions are

$$S_1(x, y, \infty) = \frac{2}{C} \sum_{k \in \mathbb{Z}^3 \setminus \{0\}} \frac{|d_k|(1 - e^{-\lambda_k t})}{|k|^{\zeta_1}} |\sin(\pi k \cdot (x - y))|.$$

up to leading order in $1/Re_\tau$ and $|k|$. We get a stationary state as $t \rightarrow \infty$, and for $|x - y|$ small,

$$S_1(x, y, \infty) = \frac{2\pi^{\zeta_1}}{C} \sum_{k \in \mathbb{Z}^3 \setminus \{0\}} |d_k| |x - y|^{\zeta_1},$$

where $\zeta_1 = 1/3 + \tau_1 \approx 0.37$. Similarly,

$$S_2(x, y, \infty) = \frac{4\pi^{\zeta_2}}{C^2} \sum_{k \in \mathbb{Z}^3 \setminus \{0\}} [d_k^2 + (\frac{C}{2})c_k] |x - y|^{\zeta_2},$$

¹The energy is $\mathcal{E} = \int_0^\infty E(k, t) dt$, $E(k, t)$ being the energy density in Fourier space.

when $|x - y|$ is small, where $\zeta_2 = 2/3 + \tau_2 \approx 0.696$, corresponding to the scaling $E(k, \infty) \sim k^{-(1+\zeta_2)}$, and

$$S_3(x, y, \infty) \sim \frac{2^3 \pi}{C^3} \sum_{k \in \mathbb{Z}^3 \setminus \{0\}} [|d_k|^3 + 3(C/2)c_k |d_k|] |x - y|^2$$

For the p th structure functions, we get the formula

$$(10) \quad S_p(x, y, t) = \frac{2^p}{C^p} \sum_{k \in \mathbb{Z}^3 \setminus \{0\}} \frac{2^{p/2} \Gamma(\frac{p+1}{2}) (\sigma_k)^p {}_1F_1(-\frac{1}{2}p, \frac{1}{2}, -\frac{1}{2}(M_k/\sigma_k)^2)}{|k|^{\zeta_p}} \times |\sin^p(\pi k \cdot (x - y))|.$$

where ${}_1F_1$ is the confluent hypergeometric function, $M_k = |d_k|(1 - e^{-\lambda_k t})$ and $\sigma_k = \sqrt{(C/2)c_k(1 - e^{-2\lambda_k t})}$, again up to leading order in $1/Re_\tau$ and $|k|$. The details of the computations of these formulas are given in [5].

The velocities in the velocity differences δu are separated by the lag variable $l = |x - y|$. One identifies three ranges for l in boundary flows:

1. The viscous range $l \ll \eta = (\nu^3/\varepsilon)^{1/4}$ where viscous forces dominate and Equations (9) does not apply.
2. The first inertial range discussed in Section 2.1 above. This is the range $\eta \ll l \ll z$, where z is the distance to the wall. The Equations (9) apply in this range. We will use this to compute the derivatives of u and the average stress, below.
3. The second inertial range due to the boundary. This is the log range $z < l < \delta$. In this range the formula (3) applies to the fluctuations and to the moments of the velocity differences as well, see [9], that have a logarithmic dependance on l/δ in this range.

4 The Moments of the Velocity Fluctuations

We will now use the solution (7) of the stochastic Navier-Stokes equation to compute the coefficients A_p in the formula (3) for the moments of the velocity fluctuations. We can write the solution as

$$u = U + u'$$

²Here S_3 is the third order structure function with absolute values inside the expectation.

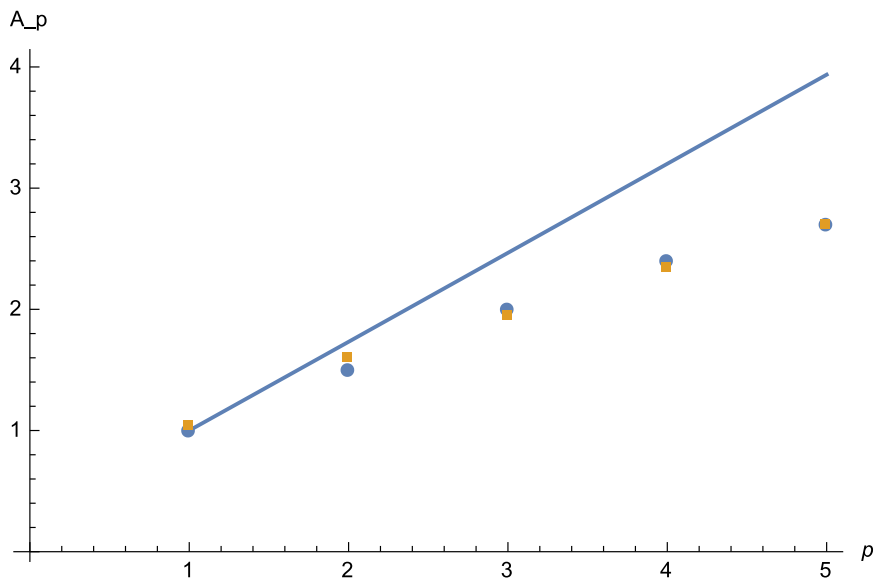


Figure 1: The first few coefficients A_p (divided by A_1) as functions of $2p$ (red squares), compared with data (blue dots), from [19], with Reynolds number $Re_\tau = 19,030$. The blue line represents the Gaussian case. The theoretical result uses a normalization of the coefficients d_k and c_k , in Equation (25), that fixes the sum of their first few symmetric functions to be one.

where U represents the (laminar) flow along the boundary and u' the turbulent part of the solutions. The arguments above indicate that U by itself is unstable for large Reynolds numbers and small perturbations grow from the boundary, so u' vanishes at the boundary and grows throughout the viscous layer. In the inertial layer u' represents the fully developed turbulence. The implications of this are that in the viscous layer

$$\frac{\partial u}{\partial y} = \frac{\partial U}{\partial y} + \frac{\partial u'}{\partial y}, \quad \left| \frac{\partial u'}{\partial y} \right| \ll 1,$$

whereas in the inertial layer

$$\frac{\partial u}{\partial y} = \frac{\partial U}{\partial y} + \frac{\partial u'}{\partial y}, \quad \left| \frac{\partial U}{\partial y} \right| \ll 1,$$

where $|\cdot|$ denotes the vector norm in \mathbb{R}^3 . We will now set the shear stress in the flow equal to

$$\tau = \nu \frac{\partial u}{\partial y}, \quad (11)$$

where u is the streamwise component of the flow, or $u = (u, v, w)$, with a slight abuse of notation. Our results both in the viscous and inertial range follow from these formulas.

It is well-known that for a laminar boundary layer flow with a small Reynolds number the streamwise velocity profile is parabolic

$$u = \frac{\tau_0 y}{\nu} \left(1 - \frac{y}{\delta}\right)$$

where $\tau_0 = \nu \frac{\partial U}{\partial y}|_{y=0}$ is the shear stress at the wall and δ is half the thickness of the boundary layer. For larger Reynolds number and turbulent flow the flow profile is linear in the viscous region closest to the wall

$$u = \frac{\tau_0}{\nu} y,$$

whereas in the inertial range it has the form

$$u = \frac{\tau_0^{1/2}}{\kappa} \log(y^+) + B,$$

where $y^+ = \frac{\tau_0^{1/2}}{\nu} y$. Both of these formulas satisfy "law of the wall", that $u = u_\tau f(y^+)$, where $u_\tau = \sqrt{\tau_0/\rho}$, but whereas the first one follows from the boundary

conditions and the Navier-Stokes equations, the second one can be derived from the energy equation in the region of fully developed turbulence, see Townsend [34]. In fact, both y dependances are the consequence of the geometry of the flow and the boundary and the symmetries of the Navier-Stokes equations, and they can be refined, see M. Oberlack [22] and Z-S. She, Y. Wu, Xi Chen and F. Hussain [32] for more information.

We will make the hypothesis, following Meneveau and Marusic [19], that the functional dependence on y can be extended to the fluctuations

$$u'^+ = \frac{u - \langle u \rangle}{u_\tau},$$

where the superscript $+$ denotes dimensionless normalization using wall units, i.e. $u'^+ = u'/u_\tau$, both in the viscous and in the inertial range. Then using the stochastic closure above we will be able to compute the coefficients A_p , in formula (3), in the inertial range. We assume, following Meneveau and Marusic [19], that the fluctuation in the inertial layer has the following scaling,

$$u'^+ \left(\frac{y}{\delta}\right) = \frac{\tau_*^{1/2}}{u_\tau} g\left(\frac{y}{\delta}\right). \quad (12)$$

where τ_* is the average stress (a random variable depend on time t); and function g describes y -dependence. Accordingly,

$$\langle (u'^+)^2 \rangle = \frac{\langle \tau_* \rangle}{u_\tau^2} g^2\left(\frac{y}{\delta}\right) \quad (13)$$

and

$$\langle (u'^+)^{2p} \rangle = \frac{\langle \tau_*^p \rangle}{u_\tau^{2p}} g^{2p}\left(\frac{y}{\delta}\right). \quad (14)$$

Therefore, we obtain the following relation

$$\langle (u'^+)^{2p} \rangle^{1/p} = \frac{\langle \tau_*^p \rangle^{1/p}}{\langle \tau_* \rangle} \langle (u'^+)^2 \rangle. \quad (15)$$

Note that if $\langle (u'^+)^2 \rangle$ is observed to display a log-law with coefficient A_1 , then $\langle (u'^+)^{2p} \rangle^{1/p}$ is also expected to display a log-law, with the coefficient

$$A_p = \frac{\langle \tau_*^p \rangle^{1/p}}{\langle \tau_* \rangle} A_1. \quad (16)$$

Since $\langle \tau_* \rangle$ (time ensemble average) is a constant, the relation between A_p and A_1 is determined by the higher order term $\langle \tau_*^p \rangle$. It is notable that if $\tau_*^{1/2}$ is Gaussian distributed, then A_p will be linear with A_1 , i.e. $A_p \rightarrow ((2p-1)!!)^{1/p} A_1$, as discussed by Meneveau and Marusic [19]. However, this disagrees with data, and a refined estimation is presented below, based on the KOSL scaling.

Our hypothesis is that in the viscous range, the streamwise velocity fluctuations have the form

$$u'^+ = \frac{\tau_*}{\nu u_\tau} y. \quad (17)$$

This is the same form as for the velocity in the viscous range above, but takes into account the normalization of the fluctuations by the friction velocity u_τ and instead of the shear stress at the wall τ_0 , the fluctuations are proportional to average shear stress in the viscous range τ_* .

In the inertial range, the above argument amounts to the hypothesis, that the streamwise fluctuations have the form

$$u'^+ = \frac{\tau_*^{1/2}}{\kappa u_\tau} \log^{1/2}(y/\delta). \quad (18)$$

(We will omit the + index for dimensionless quantities, below.) This form stems from the "attached eddy hypothesis", but uses the average shear stress τ_* in the inertial range.

We first explore the implication of (17) in the viscous range. The relation for u above in the viscous range implies that the average of the streamwise velocity is

$$\langle u \rangle = \frac{\tau_0}{\nu} y = U \quad (19)$$

since $\langle u' \rangle = 0$ in the viscous range. Thus the moments of the fluctuations in the viscous range become

$$\langle (u')^p \rangle^{1/p} = \langle \left(\frac{u-U}{u_\tau} \right)^p \rangle^{1/p} = \frac{1}{u_\tau \nu} \langle (\tau_*)^p \rangle^{1/p} y. \quad (20)$$

The solution of the stochastic Navier-Stokes equation (7) does not quite tell us how to compute the moments of the fluctuation in the viscous range because there the coefficients d_k and c_k in (6) are still growing. However, substituting $\frac{\partial U}{\partial y} + \frac{\partial u'}{\partial y}$, $|\frac{\partial u'}{\partial y}| \ll 1$, into (11), tells us that in the viscous range these moments are more similar to those of the velocity in homogeneous turbulence, see [2], than the

moments of the velocity difference $\delta u = \Delta u$ in turbulent flow, see [5]. We will see the consequences of this below.

Now we use (18) to compute the coefficients A_p in the inertial range. The formula (18) for the fluctuations implies that

$$\langle (u')^2 \rangle = B_1 - \left\langle \frac{\tau_*}{u_\tau^2 \kappa^2} \right\rangle \log(y/\delta) = D_p - \left\langle \frac{\tau_*}{u_\tau^2 \kappa^2} \right\rangle \log(y^+) \quad (21)$$

where δ is an outer length scale, that can be thickness of the boundary layer, height of a channel or radius of a pipe, $y^+ = \frac{\tau_0^{1/2}}{\nu} y$ are viscous units, and κ is the von Kármán constant. Similarly,

$$\langle (u')^{2p} \rangle^{1/p} = B_p - \frac{1}{u_\tau^2 \kappa^2} \langle (\tau_*)^p \rangle^{1/p} \log(y/\delta) = D_p - \frac{1}{u_\tau^2 \kappa^2} \langle (\tau_*)^p \rangle^{1/p} \log(y^+) \quad (22)$$

in the inertial range. The coefficients B_1 (B_p) are determined by the boundary conditions at the end of the inertial range. We will now use the Formula (7) to compute $\langle (\tau_*)^p \rangle^{1/p}$ in the inertial range. This permits us to compute the coefficients in Equations (3) and (22)

$$A_p = \frac{1}{u_\tau^2 \kappa^2} \langle (\tau_*)^p \rangle^{1/p}. \quad (23)$$

This is consistent with equation (16).

We start with the assumption that the average strain is proportional to the y derivative of the velocity at some point (y^*) in the inertial range: $\tau_* = \nu \frac{\partial u^*}{\partial y}$. Then by the mean-value theorem

$$\tau_* = \nu \frac{\partial u^*}{\partial y} = \nu \frac{u(y^* + l^*) - u(y^*)}{l^*}$$

where l^* is some small value of the lag variable l , or

$$\langle (\tau_*)^p \rangle^{1/p} = \left\langle \left[\nu \frac{u(y^* + l^*) - u(y^*)}{l^*} \right]^p \right\rangle^{1/p} = \nu \frac{1}{l^{*p}} [C_p(\ell^*) \zeta_p]^{1/p} = \nu C_p^{1/p}(\ell^*) \zeta_p^{1/p-1}$$

using the Kolmogorov-Obukhov-She-Leveque formula (9), where l^* is now a small number. This formula applies to the distances l^* in mean-value theorem, see discussion in Section 3. This now gives the formulas

$$A_1 = \frac{\nu}{\kappa^2 \tau_0} C_1 \left(\frac{1}{l^*} \right)^{1-\zeta_1},$$

and

$$A_p = \frac{\mathbf{v}}{\kappa^2 \tau_0} C_p^{1/p} \left(\frac{1}{l^*} \right)^{1 - \frac{\zeta_p}{p}}, \quad (24)$$

so

$$A_p = \frac{C_p^{1/p}}{C_1} \left(\frac{1}{l^*} \right)^{\zeta_1 - \frac{\zeta_p}{p}} A_1. \quad (25)$$

We also get that

$$A_p \rightarrow \left(\frac{1}{l^*} \right)^{\zeta_1 - 1/9} \frac{C_p^{1/p}}{C_1} A_1 \rightarrow b \sqrt{p} A_1,$$

as $p \rightarrow \infty$, where b is a constant. Indeed, the formulas for the structure functions above give values for the limit,

$$\frac{C_p^{1/p}}{C_1} = \frac{1}{\pi^{\zeta_1 - \zeta_p/p}} \times \frac{[\sum_{k \in \mathbb{Z}^3 \setminus \{0\}} 2^{p/2} \Gamma(\frac{p+1}{2}) (\sqrt{(C/2)c_k})^p {}_1F_1(-\frac{1}{2}p, \frac{1}{2}, -\frac{1}{2}(|d_k|^2/(C/2)c_k))]^{1/p}}{\sum_{k \in \mathbb{Z}^3 \setminus \{0\}} |d_k|},$$

so

$$\left(\frac{1}{l^*} \right)^{\zeta_1 - \zeta_p/p} \frac{C_p^{1/p}}{C_1} \leq \frac{1}{(\pi l^*)^{\zeta_1 - \zeta_p/p}} \frac{\left(\sum_{k \in \mathbb{Z}^3 \setminus \{0\}} ((C/2)c_k + d_k^2) \right)^{1/2}}{\sum_{k \in \mathbb{Z}^3 \setminus \{0\}} |d_k|} (\Gamma(\frac{p+1}{2}))^{1/p} \sim b \sqrt{p},$$

for p large, using the asymptotics of the Gamma function, for p large,

$$(\Gamma(\frac{p+1}{2}))^{1/p} \sim \left(\frac{4\pi}{p+1} \right)^{1/2p} \left(\frac{p+1}{2e} \right)^{1/2 + 1/2p} \left(1 + O\left(\frac{2}{p+1} \right) \right)^{1/p},$$

with the coefficient

$$b = \frac{1}{(\pi l^*)^{\zeta_1 - 1/9} \sqrt{2e}} \frac{\left(\sum_{k \in \mathbb{Z}^3 \setminus \{0\}} ((C/2)c_k + d_k^2) \right)^{1/2}}{\sum_{k \in \mathbb{Z}^3 \setminus \{0\}} |d_k|}.$$

The first few coefficients A_p are shown in Figure 1, where they are compared with high Reynolds number data, see [19]. We conclude that if $l^* > 0$, then all the A_p are bounded, for finite p .

This shows that the sub-Gaussian behavior of the coefficients A_p , as p increases, is caused by the KOSL scaling.

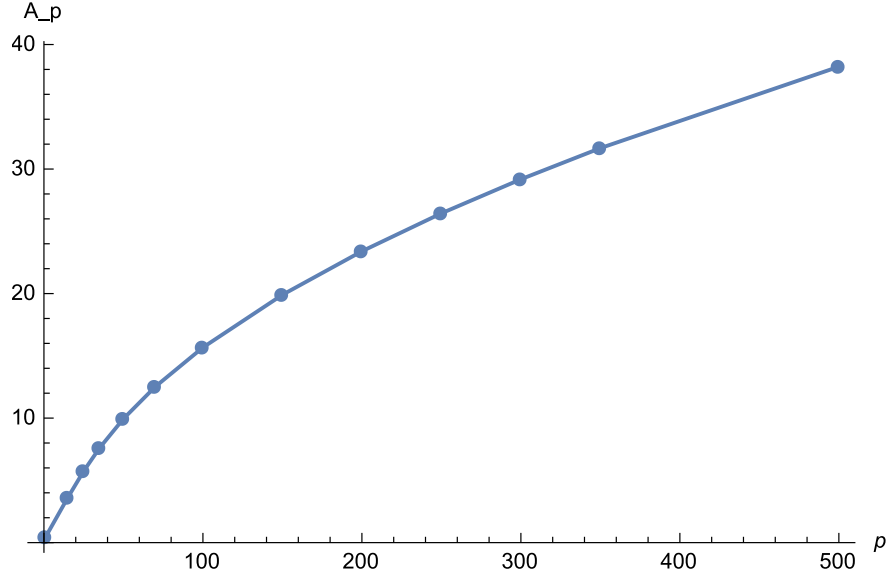


Figure 2: The coefficients A_p for large values of p . The value of l^* is the same as in Figure 1, but in addition the normalizations of the coefficients d_k and c_k , in Figure 1, fix the asymptotic coefficient b .

The underestimate

$$\left(\frac{1}{l^*}\right)^{\zeta_1 - \zeta_p/p} \frac{C_p^{1/p}}{C_1} \geq \frac{1}{(\pi l^*)^{\zeta_1 - \zeta_p/p} \sqrt{2e}} \frac{\left(\sum_{k \in \mathbb{Z}^3 \setminus \{0\}} ((C/2)c_k)^{p/2}\right)^{1/p}}{\sum_{k \in \mathbb{Z}^3 \setminus \{0\}} |d_k|} \sqrt{p},$$

for p large, gives us the limit

$$A_\infty = \lim_{p \rightarrow \infty} A_p = \infty. \quad (26)$$

Figure 2 shows the asymptotics of A_p to $b\sqrt{p}A_1$, for large p .

5 The invariant measure of the stochastic Navier-Stokes

The integral equation (7) can be considered to be an infinite-dimensional Ito process, see [6]. This means that we can find the associated Kolmogorov backward

equation for the Ito diffusion associated with the equation (7) and this equations that determines the invariant measure of turbulence, see [5], is linear. This was first attempted by Hopf [11] wrote down a functional differential equation for the characteristic function of the invariant measure of the deterministic Navier-Stokes equation. The Kolmogorov-Hopf (backward) equation for (7) is

$$\frac{\partial \phi}{\partial t} = \frac{1}{2} \text{tr}[P_t C P_t^* \Delta \phi] + \text{tr}[P_t \bar{D} \nabla \phi] + \langle K(z) P_t, \nabla \phi \rangle, \quad (27)$$

see [5] and [6] Chapter 3, where $\bar{D} = (|k|^{1/3} D_k)$, $\phi(z)$ is a bounded function of z , $P_t = e^{-\int_0^t \nabla u \, dr} M_t \prod_k^m |k|^{2/3} (2/3)^{N_t^k}$. The variance and drift are defined to be

$$Q_t = \int_0^t e^{K(s)} P_s C P_s^* e^{K^*(s)} ds, \quad E_t = \int_0^t e^{K(s)} P_s \bar{D} ds. \quad (28)$$

In distinction to the nonlinear Navier-Stokes equation (6) that cannot be solved explicitly, the linear equation (27) can be solved. The solution of the Kolmogorov-Hopf equation (27) is

$$R_t \phi(z) = \int_H \phi(e^{Kt} P_t z + EI + y) \mathcal{N}_{(0, Q_t)} * \mathbb{P}_{N_t}(dy),$$

\mathbb{P}_{N_t} being the law of the log-Poisson process (8). The invariant measure of turbulence that appears in the last equation can now be expressed explicitly, The invariant measure of the Navier-Stokes equation on $H_c = H^{3/2+}(\mathbb{T}^3)$ is

$$\mu(dx) = e^{\langle Q^{-1/2} EI, Q^{-1/2} x \rangle - \frac{1}{2} |Q^{-1/2} EI|^2} \mathcal{N}_{(0, Q)}(dx) \sum_k \delta_{k, l} \prod_{j \neq l}^m \delta_{N_t^j} \sum_{j=0}^{\infty} p_{m_l}^j \delta_{(N_l - j)}, \quad (29)$$

where $Q = Q_\infty$, $E = E_\infty$, $m_k = \ln |k|^{2/3}$ is the mean of the log-Poisson processes (8) and $p_{m_k}^j = \frac{(m_k)^j e^{-m_k}}{j!}$ is the the probability of $N_\infty^k = N_k$ having exactly j jumps, $\delta_{k, l}$ is the Kroncker delta function.

This shows that the invariant measure of turbulence is simply a product of two measure, one an infinite-dimensional Gaussian that gives the Kolmogorov-Obukhov scaling and the other a discrete Poisson measure that gives the She-Leveque intermittency corrections. Together they produce the scaling of the structure functions in Equation (9).

The quantity that can be compared directly to experiments is the probability density function (PDF) of either the velocity u or the velocity differences δu . We

take the trace of the Kolmogorov-Hopf equation (27), see [6] Chapter 3, to compute the differential equation satisfied by the PDE. First we do this ignoring the intermittency corrections τ_p in Equation (9), see [7] for details. The stationary equation satisfied by the PDF without intermittency corrections is

$$\frac{1}{2}\phi_{rr} + \frac{1+|c|}{r}\phi_r = \frac{1}{2}\phi. \quad (30)$$

6 The Probability Density Function (PDF)

The PDF, without intermittency corrections, is a Generalized Hyperbolic Distribution (GID) of Barndorff-Nielsen [1]:

$$f(x) = \frac{(\gamma/\delta)^\lambda}{\sqrt{2\pi}K_\lambda(\delta\gamma)} \frac{K_{\lambda-\frac{1}{2}}\left(\alpha\sqrt{\delta^2 + (x-\mu)^2}\right) e^{\beta(x-\mu)}}{\left(\sqrt{\delta^2 + (x-\mu)^2}/\alpha\right)^{\lambda-\frac{1}{2}}} \quad (31)$$

where K_λ is modified Bessel's function of the second kind with index λ , $\gamma = \sqrt{\alpha^2 - \beta^2}$. α, β, δ and μ are parameters. (31) is the solution of (30), see [7] for details of the proof, and the PDF that can be compared a large class of experimental data.

The PDF becomes more complicated when the intermittency is included. Then it becomes impossible to have a single PDF for all the different moments and instead one has to have a distribution that is a product of a discrete and continuous distributions. One can put in the intermittency correction in the equation (30) defining the PDF and get different PDF for each moment, this is done in [7]. In [8] a different approach was taken and the invariant measure (29) projected to a PDF that is a product of a continuous and a discrete measure analogous to the invariant measure itself. The continuous part of the PDF is the Generalized Hyperbolic Distribution (31).

Following [8], we start with the log-Poisson process $|x| \left(\frac{2}{3}\right)^{N_t^k}$ and the mean $m_k = \ln(|x|^{-6})$ of the associated Poisson distribution. Now the mixed continuous and discrete distribution is given by:

$$\bar{\mu}(\cdot) = \int_{-\infty}^{\infty} \sum_{j=0}^{\infty} \frac{(\ln(|x|^{-6}))^j}{j!} |x|^6 \delta_{N_t^k - j}(\cdot) f(x) dx, \quad (32)$$

where $\bar{\mu}$ denotes the projection of the measure (29). We assume that the velocity is a Hölder continuous function of Hölder index 1/3, see [6]. Then evaluating the

measure on the p th moment of the velocity differences gives,

$$\begin{aligned} \int_{-\infty}^{\infty} \sum_{j=0}^{\infty} \frac{(\ln(|x|^{-6}))^j}{j!} |x|^6 \delta_{N_t^k - j}(|x| \left(\frac{2}{3}\right)^{N_t^k})^{\frac{p}{3}} f(x) dx &= \int_{-\infty}^{\infty} |x|^{\frac{p}{3}} |x|^{6(1-(2/3)^{\frac{p}{3}})} f(x) dx \\ &= \int_{-\infty}^{\infty} |x|^{p+3\tau_p} f(x) dx = \int_{-\infty}^{\infty} |x|^{3\xi_p} f(x) dx, \end{aligned}$$

where

$$\xi_p = \frac{p}{3} + \tau_p$$

is the scaling exponent (9) of the p th structure function, with the intermittency correction τ_p . The upshot is that the discrete part of the PDF adds the intermittency correction $|x|^{3\tau_p}$ to the p th moment and

$$\bar{\mu}(|\delta u|^p) = \int_{-\infty}^{\infty} |x|^{p+3\tau_p} f(x) dx, \quad (33)$$

where δu are the velocity differences and the intermittency corrections are $\tau_p = 2(1 - (2/3)^{\frac{p}{3}})$.

Thus to recap, the PDF for the velocity differences in turbulent flow is a product of a discrete and a continuous measure:

$$d\mu = \sum_{j=0}^{\infty} \frac{(\ln(|x|^{-6}))^j}{j!} |x|^6 \delta_{N_t^k - j}(\cdot) f(x) dx, \quad (34)$$

where dx denotes Lebesgue measure and $f(x)$ is the Generalized Hyperbolic Distribution (31). The evaluation of this measure on the p th power of the absolute value of the velocity differences $|\delta u|^p$ gives the continuous measure

$$d\eta = |x|^{3\xi_p} f(x) dx,$$

where again $f(x)$ is given by (31).

7 The PDF of the Fluctuations

In this section, we use DNS data to check above analysis. The DNS database used for comparison in this paper is built by solving the three-dimensional Navier-Stokes equations for an incompressible turbulent channel flow. The equation of

motion have been discretized using a staggered central second-order finite difference scheme in an orthogonal coordinate system based on a fractional step and factorization method [24]. A third-order Runge-Kutta scheme is used to advance the equations in time. Moreover, a mean parabolic velocity profile with random fluctuations is used as an initial condition in the entire domain to trigger turbulence until a fully developed turbulent channel flow is reached. Periodic boundary conditions are used along the spanwise and streamwise directions, and isothermal condition is applied for the walls. In the present study, a constant flow rate is imposed by applying an external force due to energy dissipation. The Reynolds number in this study is 394, $Re_\tau = u_\tau h/\nu$, where ν is the kinematic viscosity and u_τ is the friction velocity of the channel flow. The dimension of the computational box are selected as follows: $L_z = \pi h$, $L_y = 2h$ and $L_x = 8\pi h$, where h is the length of half channel. A grid-independence test was performed and details are given in [16]. The mesh configuration is: $193 \times 193 \times 1153$, which represent the numbers of points along the spanwise (z), normal (y) and streamwise (x) directions, respectively. The present DNS data is validated by comparing with other DNS data as shown in figures below. It can be seen from Figure 3 that the mean streamwise velocity of the present study has a very good agreement with other DNS data at similar Reynolds numbers, and the present velocity fluctuation distributions also show fairly good agreements. This fact confirms the acceptable resolution of the selected mesh configuration and quality of simulations.

Then from the vantage point of homogeneous turbulence, see [2], the above analysis of the coefficients A_p can be interpreted to say that the fluctuations of the fluid velocity have the properties of velocity differences in the inertial layer but of velocity, in homogeneous turbulence, in the viscous layer. We now confirm this by computing the PDF for the fluctuations in those two layers. The PDF in the inertial layer are well modeled by the Generalized Hyperbolic Distributions (GHD) above, whereas the PDF in the viscous layers are skewed-Gaussians, see Figure 4. The normalized velocity gradient

$$\frac{du^+}{dy^+} = \frac{\nu}{u_\tau^2} \frac{du}{dy} \approx \frac{\nu}{u_\tau^2} \frac{\Delta u}{\Delta y}$$

has similar properties as the fluctuations. We will compare the PDFs of the velocity gradient to the NIG distributions based on direct numeric simulation of Navier-Stokes equation (The NIG is a special case of the GHD and the parameters δ and α of GHD can be adjusted to closely approximate the NIG.)

The comparison between DNS data and theoretical results are shown in Figure 5 and below.

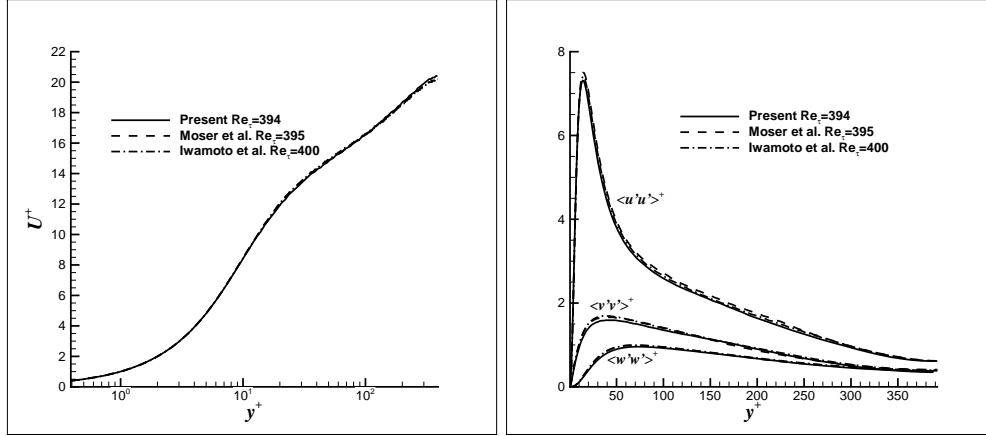


Figure 3: Current DNS results (solid line - [16]) compared with previous simulations in literatures (dashed line - [21]; dashed dotted line - [13]) showing good agreements with each other. [left] Mean velocity $U^+ = U/u_\tau$ as a function of wall distance y^+ . [right] Turbulent kinetic energy in different directions, $\langle u'u' \rangle^+$, $\langle v'v' \rangle^+$, $\langle w'w' \rangle^+$ as function of y^+ .

We see that in the inertial range the PDFs are similar to the PDFs of turbulent velocity differences δu (31) but in the viscous range, the PDF are similar (except for their skewness) to the PDFs of the velocity in homogeneous turbulence. This confirms the above observations.

8 Conclusions

We have derived the generalized log-law for the fluctuations in boundary-value flows, in the inertial range,

$$\langle (u')^{2p} \rangle^{1/p} = B_p - A_p \ln(y/\delta) = D_p(Re_\tau) - A_p \ln(y^+), \quad (35)$$

suggested by Meneveau and Marusic [19] and inspired by the log-law of the second moment of the fluctuations [18, 12, 17, 20]. The ideas that go into the derivation are simple, first the attached eddy hypothesis [34] says that the number of eddies decreases as one over the distance to the wall, as we move away from the wall. This gives the logarithmic dependence of the variance on the distance to the

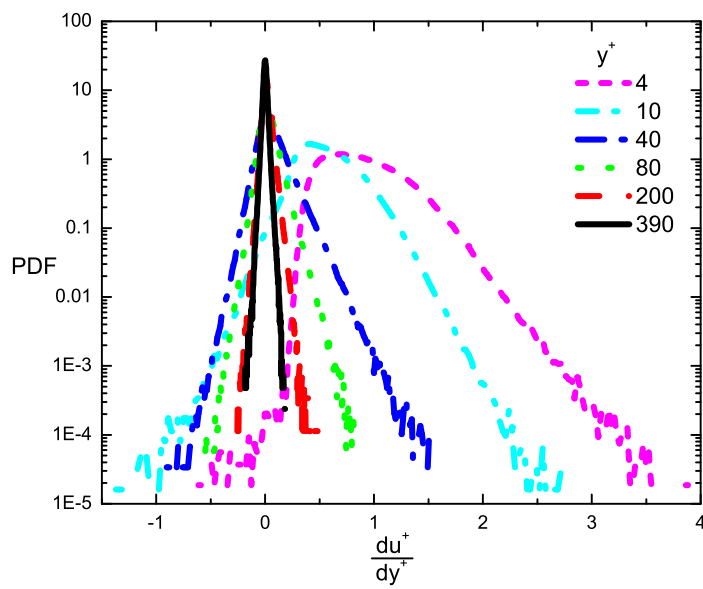


Figure 4: A comparison of the PDFs (in the log-linear coordinate) for the fluctuation in the inertial and viscous range. Channel flow at $Re_\tau=390$. PDFs of velocity gradient at different y^+ locations

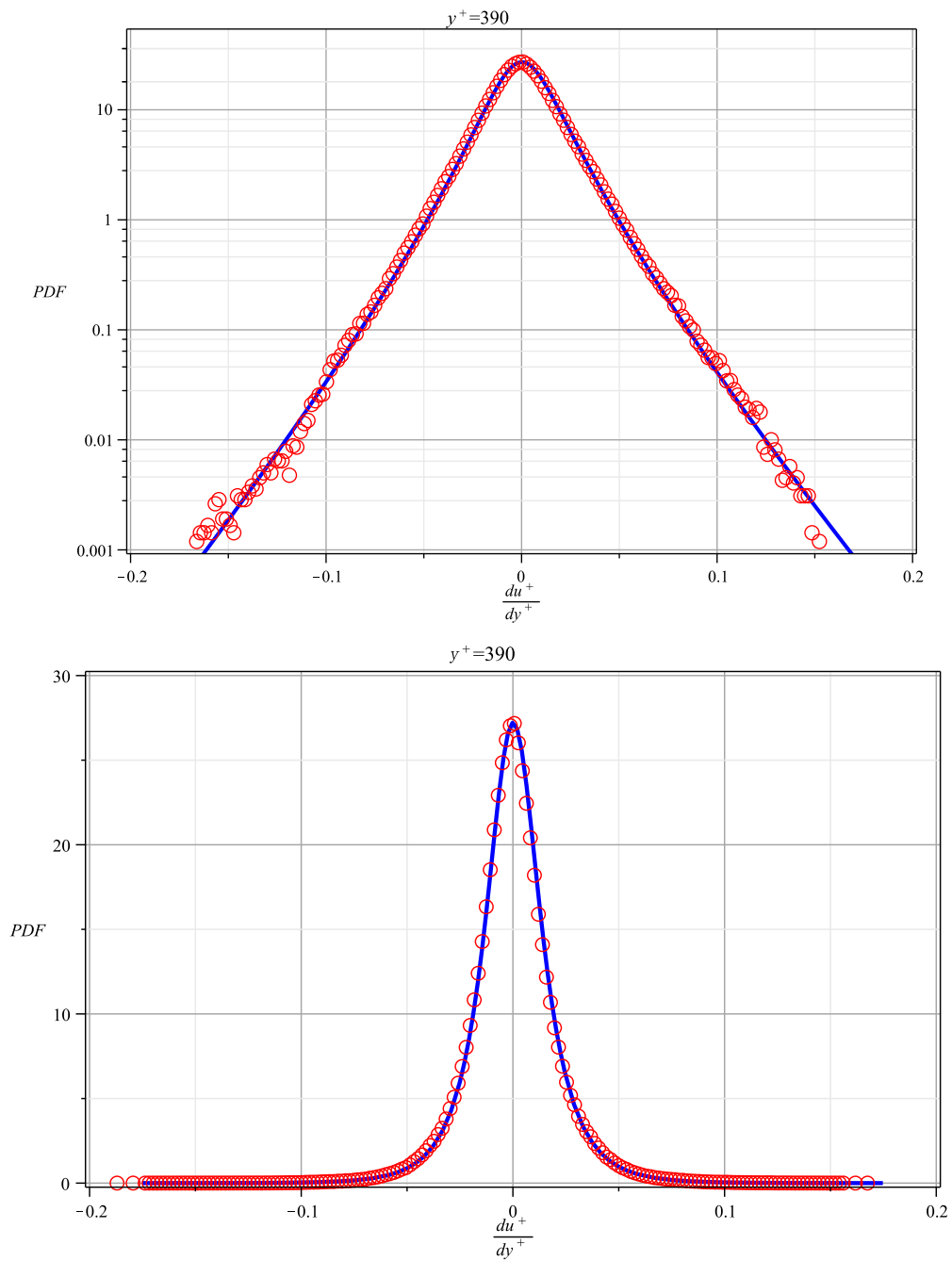


Figure 5: PDF of velocity gradient at $y^+ = 390$. Red: DNS data; Blue: GHD. [up] log-linear coordinate; [bottom] linear-linear coordinate.

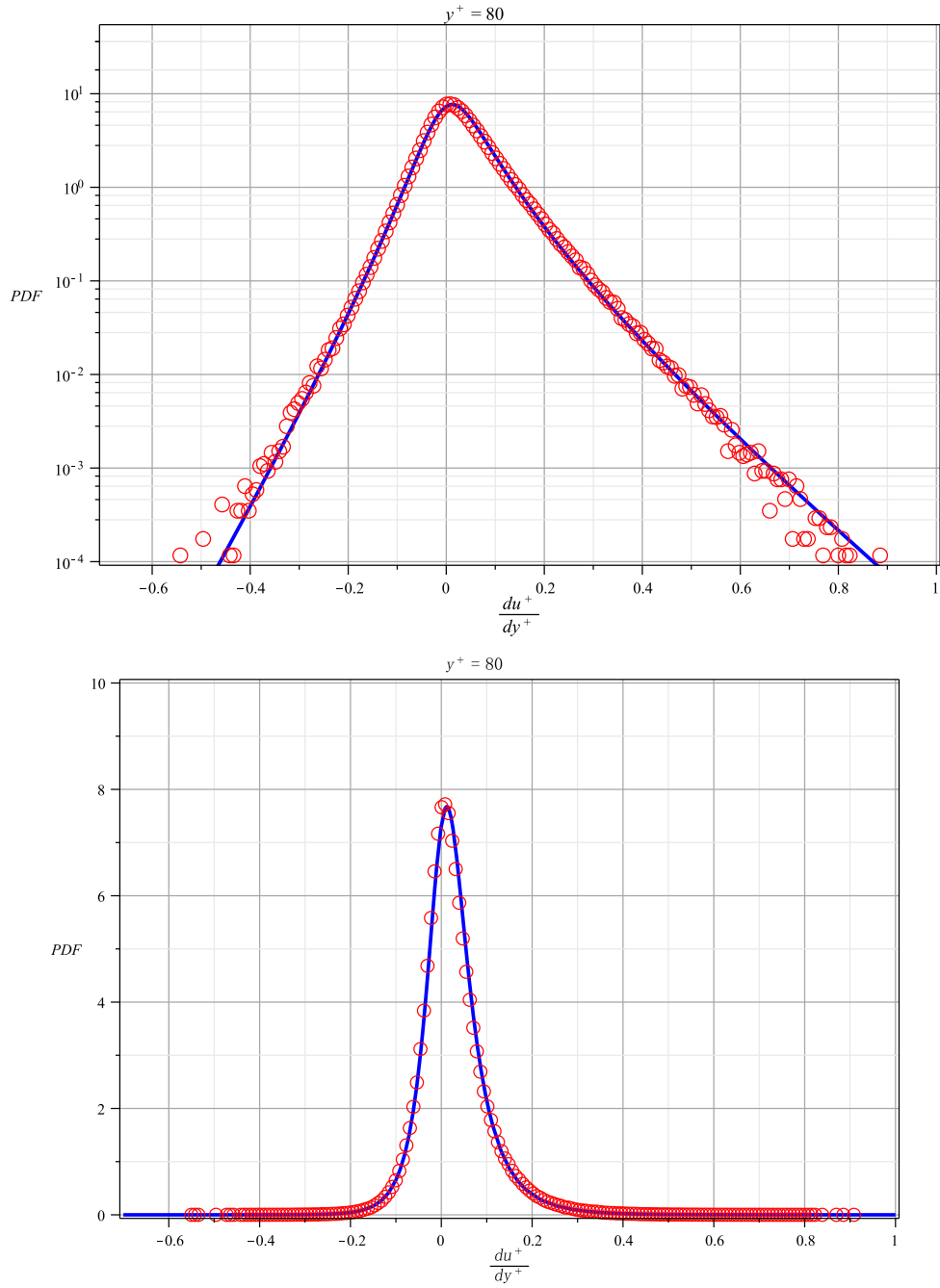


Figure 6: PDF of velocity gradient at $y^+ = 80$. Red: DNS data; Blue: GHD. [up] log-linear coordinate; [bottom] linear-linear coordinate.

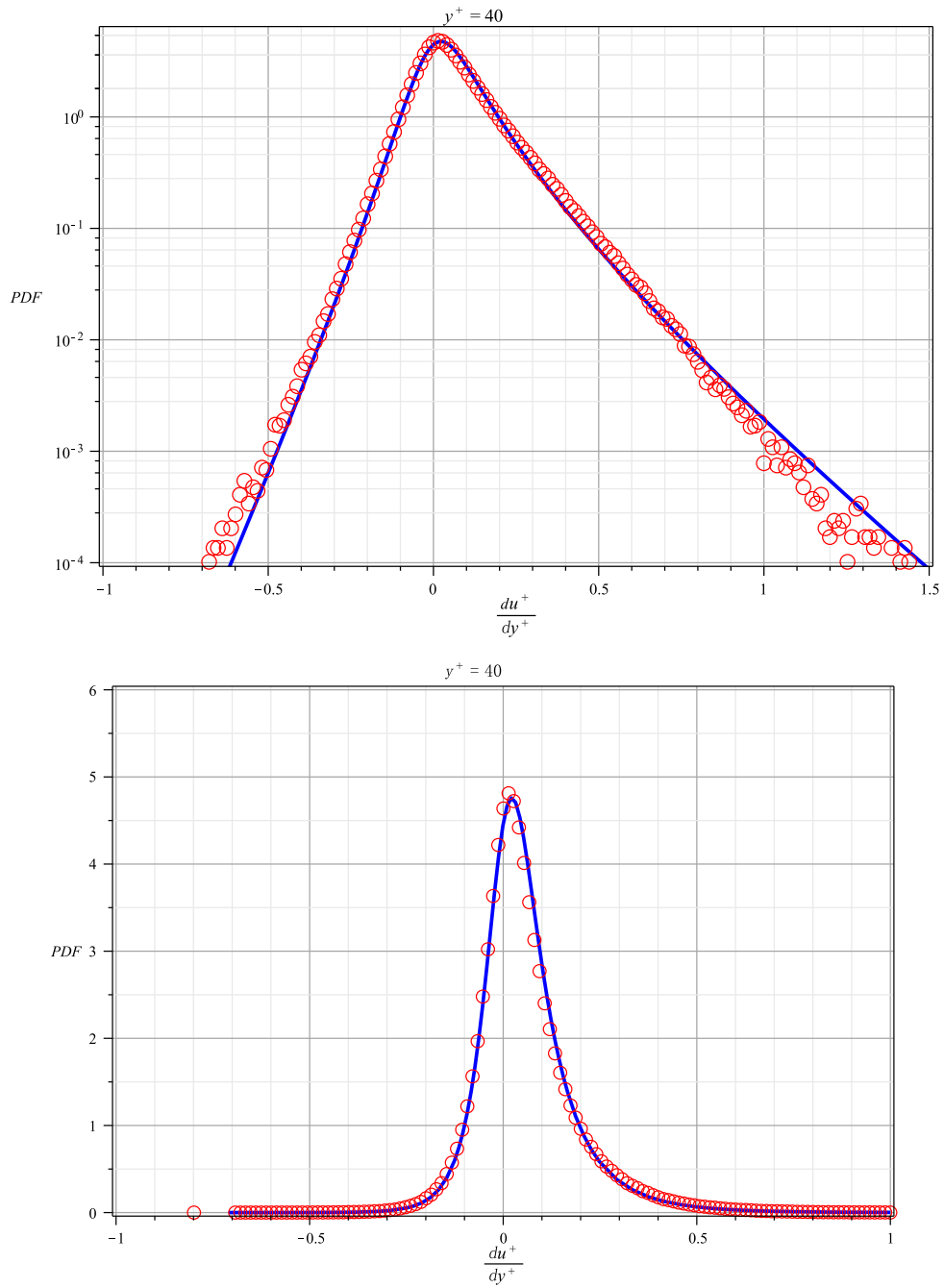


Figure 7: PDF of velocity gradient at $y^+ = 40$. Red: DNS data; Blue: GHD. [up] log-linear coordinate; [bottom] linear-linear coordinate.

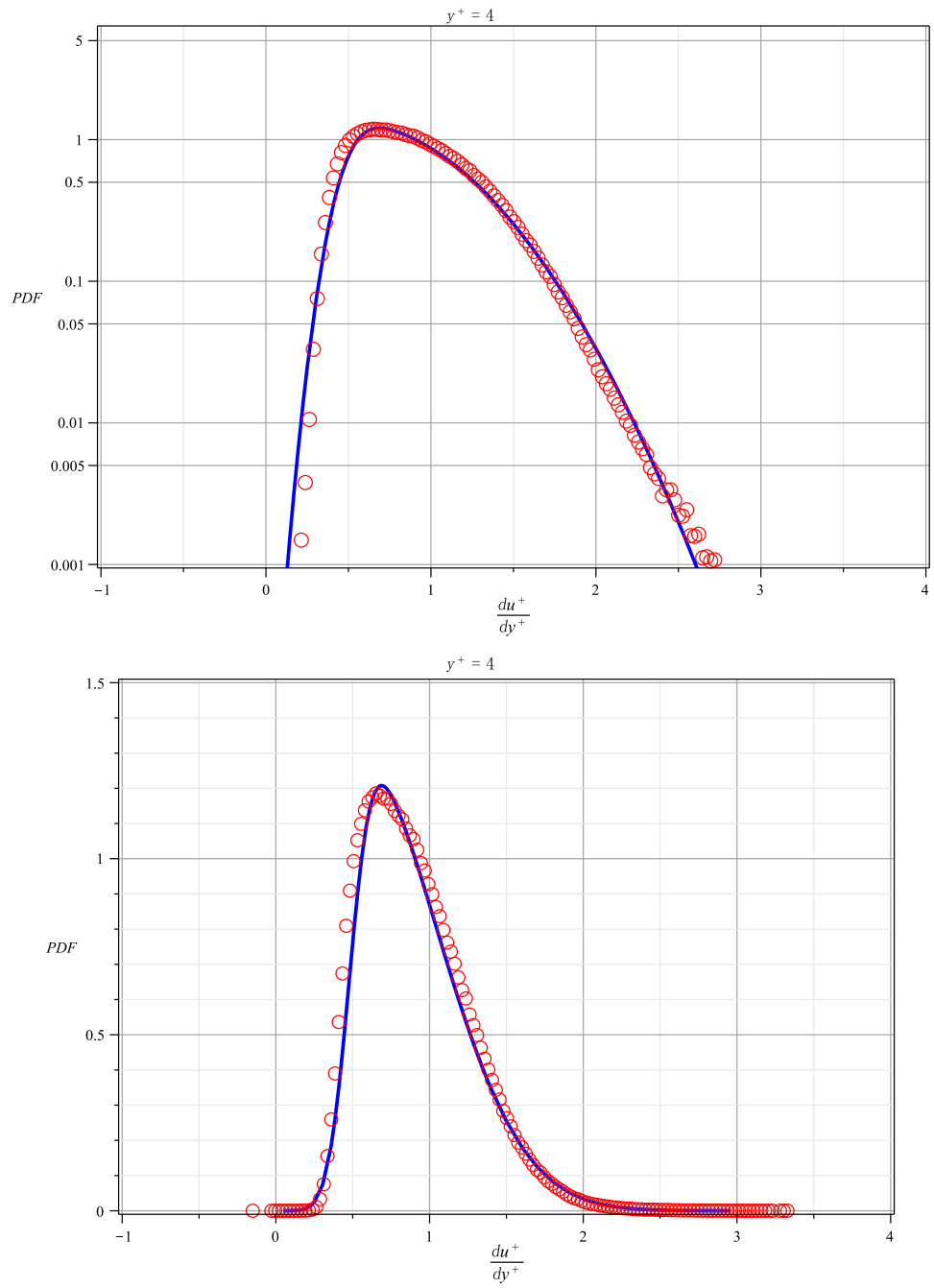


Figure 8: PDF of velocity gradient at $y^+ = 4$. Red: DNS data; Blue: Skew-Gaussian. [up] log-linear coordinate; [bottom] linear-linear coordinate.

wall, see [34]. Then we assume a "law of the wall" for the fluctuations

$$u'^+ \left(\frac{y}{\delta} \right) = \frac{\tau_*^{1/2}}{u_\tau} g \left(\frac{y}{\delta} \right) \quad (36)$$

where τ_* is the average shear stress in the inertial range. This relation gives the relation

$$\frac{A_p}{A_1} = \frac{\langle \tau_*^p \rangle^{1/p}}{\langle \tau_* \rangle}. \quad (37)$$

for the coefficients A_p . The third idea is to use that the averaged shear stress in the inertial range is give by the Kolmogorov-Obukhov scaling of the structure functions of the velocity differences, with the She-Leveque intermittency corrections. The final idea is to use the stochastic closure theory of Birnir [5, 6] to compute the coefficients A_p

$$A_p = \left(\frac{1}{l^*} \right)^{\zeta_1 - \zeta_p/p} \frac{C_p^{1/p}}{C_1} A_1$$

where $\zeta_p = p/3 + \tau_p = p/9 + 2(1 - (2/3)^{p/3})$ are the Kolmogorov-Obukhov-She-Leveque (KOSL), scaling exponents and the coefficients C_p are given in terms of the mean and variance of the turbulent velocity, see (10). These coefficients are the raw-moments of a Gaussian. The sub-Gaussian behavior of the coefficients A_p is given by an interplay between the function $\left(\frac{1}{l^*} \right)^{\zeta_1 - \zeta_p}$ produced by the KOSL scaling and the "square root of Gaussian" behavior of the coefficients C_p . As p become large the former function approaches a constant in p : $\left(\frac{1}{l^*} \right)^{\zeta_1 - 1/9}$, whereas $C_p/C_1 \sim b\sqrt{p}$, where b is a constant. The Gaussian behavior would be $A_p/A_1 \sim cp$, where c is a constant. In particular, $\lim_{p \rightarrow \infty} A_p = \infty$. Thus the sub-Gaussian behavior for p large is caused by the formulas (36) and (37); that the variance of the fluctuations is proportional to $\langle \tau_*^p \rangle$ but not $\langle \tau_*^{2p} \rangle$.

The PDFs for the velocity moments in homogeneous turbulence are well-known to be Gaussians, see [2, 34], whereas the PDFs of the structure function of velocity differences are Generalized Hyperbolic Distributions with intermittency corrections (33), see [5, 6, 8]. We showed that the PDFs of the moments of the fluctuations in the viscous range are similar to the former, except for also being skewed, whereas they are similar to the latter in the inertial range.

One can also use the stochastic closure theory in [5, 6] to compute the Reynolds number dependance of the moments of the fluctuations (35) but this will be done in another publication.

Acknowledgements

The first author was supported by a grant from the UC Santa Barbara Academic Senate and by the University of Iceland Science Faculty, both of which are gratefully acknowledged. The research was also partially supported by a Chair of Excellence at Carlos III, University Madrid, in Spring of 2015, for which the first author wants to express his gratitude.

References

- [1] O. E. Barndorff-Nielsen. Exponentially decreasing distributions for the logarithm of the particle size. *Proc. R. Soc. London, A* 353:401–419, 1977.
- [2] G. K. Batchelor. *The Theory of Homogenous Turbulence*. Cambridge Univ. Press, New York, 1953.
- [3] P. S. Bernard and J. M. Wallace. *Turbulent Flow*. John Wiley & Sons, Hoboken, NJ, 2002.
- [4] B. Birnir. Turbulence of a unidirectional flow. *Proceedings of the Conference on Probability, Geometry and Integrable Systems, MSRI, Dec. 2005 MSRI Publications, Cambridge Univ. Press*, 55, 2007. Available at <http://repositories.cdlib.org/cnls/>.
- [5] B. Birnir. The Kolmogorov-Obukhov statistical theory of turbulence. *J. Nonlinear Sci.*, 2013. DOI 10.1007/s00332-012-9164-z.
- [6] B. Birnir. *The Kolmogorov-Obukhov Theory of Turbulence*. Springer, New York, 2013.
- [7] B. Birnir. The Kolmogorov-Obukhov-She-Leveque scaling in turbulence. *Communications on Pure and Applied Analysis*, 13(5), 2014.
- [8] B. Birnir. From wind blown sand to turbulence and back. *The fascination of Probability, Statistics and Their Applications*, eds A. Veraart, S.Thorbjornsen, R. Stelzer and M. Podolskij, Springer-Verlag New York, 2015.

- [9] J. D. Woodcock C. M de Silva, I. Marusic and C. Meneveau. Scaling of second- and higher-order structure functions turbulent boundary layers. *J. Fluid Mech.*, 769:654–686, 2015.
- [10] B. Dubrulle. Intermittency in fully developed turbulence: in log-Poisson statistics and generalized scale covariance. *Phys. Rev. Letters*, 73(7):959–962, 1994.
- [11] E. Hopf. Statistical hydrodynamics and functional calculus. *J. Rat. Mech. Anal.*, 1(1):87–123, 1953.
- [12] M. Hultmark, M Vallikivi, S.C.C. Bailey, and A. J. Smits. Turbulent pipe flow at extreme reynolds numbers. *Phys. Rev. Lett.*, 108(9):94501, 2012.
- [13] K. Iwamoto, Y. Suzuki, and Kasagi N. Database of fully developed channel flow. (ILR-0201, see <http://www.thtlab.t.utokyo.ac.jp/>), 2002.
- [14] J. Jimenez. Cascades in wall-bounded turbulence. *Annu. Rev. Fluid Mech.*, 44:27–45, 2012.
- [15] A. N. Kolmogorov. A refinement of previous hypotheses concerning the local structure of turbulence in a viscous incompressible fluid at high Reynolds number. *J. Fluid Mech.*, 13:82–85, 1962.
- [16] Can Liu. Direct numerical simulations (dns) of the thermal field in a turbulent channel flow with spanwise sinusoidal blowing/suction. *M.S. Thesis, Texas Tech University*, 2013.
- [17] I. Marusic. The logarithmic region of wall turbulence: universality, structure and interactions. In *Proceedings of 18th Australasian Fluid Mechanics Conference, 3rd-7th December 2012 (ed. P. A. Brandner & B. W. Pearce). Australasian Fluid Mechanics Society.*, 2012.
- [18] I. Marusic and G. J. Kunkel. Streamwise turbulence intensity formulation for flat-plate boundary layers. *Phys. Fluids*, 15:2461–2464, 2003.
- [19] I. Marusic and C. Meneveau. Generalized logarithmic law for high-order moments in turbulent boundary layers. *J. Fluid Mech.*, 719, R1:1–11, 2013.
- [20] I. Marusic, J. P. Monty, M. Hultmark, and A. J. Smits. On the logarithmic region in wall turbulence. *J. Fluid Mech.*, 716, R3, 2013.

- [21] R.D. Moser, J. Kim, and N.N. Mansour. Direct numerical simulation of turbulent channel flow up to $\text{Re}_\tau = 590$. *Phys. Fluids*, 943, 1999.
- [22] M. Oberlack. A unified approach for symmetries in plane parallel turbulent shear flow. *J. Fluid Mech.*, 427:299–328, 2001.
- [23] A. M. Obukhov. Some specific features of atmospheric turbulence. *J. Fluid Mech.*, 13:77–81, 1962.
- [24] P. Orlandi. Fluid flow phenomena : A numerical toolkit. *Dordrecht, Kluwer*, 2000.
- [25] A. E. Perry and M. S. Chong. On the mechanism of wall turbulence. *J. Fluid Mech.*, 119:173–217, 1982.
- [26] A. E. Perry and M. S. Chong. A theoretical and experimental study of wall turbulence. *J. Fluid Mech.*, 165:163–199, 1986.
- [27] L. Prandtl. Bericht ueber Untersuchungen zur ausgebildeten Turbulenz. *Z. Angew. Math. Mech.*, 5:136–139, 1925.
- [28] O. Reynolds. An experimental investigation of the circumstances which determine whether the motion of water shall be direct or sinuous, and the the law of resistance in parallel channels. *Phil. Trans. Roy. Soc. Lond.*, 174(11):935–982, 1883.
- [29] O. Reynolds. On the dynamical theory of incompressible viscous fluids and the determination of the criterion. *Phil. Trans. Roy. Soc. Lond.*, 186A:123–164, 1885.
- [30] Z-S She and E. Leveque. Universal scaling laws in fully developed turbulence. *Phys. Rev. Letters*, 72(3):336–339, 1994.
- [31] Z-S She and E. Waymire. Quantized energy cascade and log-poisson statistics in fully developed turbulence. *Phys. Rev. Letters*, 74(2):262–265, 1995.
- [32] Z-S She, Y. Wu, Xi Chen, and F. Hussain. A multi-scale description of roughness effects in turbulent pipe flow. *New Journal of Physics*, 14:093054, 2012.
- [33] A. J. Smits, McKeon B. J., and I. Marusic. High-reynolds number wall turbulence. *Annu. Rev. Fluid Mech.*, 43:353–75, 2011.

- [34] A. A. Townsend. *The Structure of Turbulent Flow*. Cambridge Univ. Press, New York, 1976.
- [35] T. von Kármán. Mechanische Ähnlichkeit und Turbulenz. *Proceedings of the Third International Congress for Applied Mechanics, Sveriges Lotografiska Tryckeriet Stocholm*, 1:79–73, 1994.